



Fetoscopic insufflation modeled in the extrauterine environment for neonatal development (EXTEND): Fetoscopic insufflation is safe for the fetus[☆]



Barbara E. Coons^{a,1}, Kendall M. Lawrence^{a,1}, Ryne Didier^b, Anush Sridharan^b, James K. Moon^a, Avery C. Rossidis^a, Heron D. Baumgarten^a, Aimee G. Kim^a, Ali Y. Mejaddam^a, Katsusuke Ozawa^a, Felix De Bie^a, Marcus Davey^a, Alan W. Flake^{a,*}

^a Center for Fetal Research, Children's Hospital of Philadelphia, Philadelphia, Pennsylvania, USA

^b Department of Radiology, Children's Hospital of Philadelphia, Philadelphia, Pennsylvania, USA

ARTICLE INFO

Article history:

Received 21 September 2020

Accepted 23 September 2020

Key words:

Fetal surgery

Fetoscopic

Partial amniotic CO₂ insufflation

Contrast enhanced ultrasound

ABSTRACT

Background: Minimally invasive fetal surgery, or fetoscopy, is an alternative to open fetal surgery to repair common birth defects like myelomeningocele. Although this hysterotomy-sparing approach reduces maternal morbidity, the effects of *in utero* insufflation on the fetus are poorly understood. Our purpose was to determine the optimal fetal insufflation conditions.

Methods: Fetal sheep at gestational age 104 to 107 days were studied under insufflation conditions *in utero* and *ex utero*. The *ex utero* fetuses were cannulated via their umbilical vessels into a support device, the EXTra-uterine Environment for Neonatal Development (EXTEND). EXTEND fetuses were exposed to four different insufflation conditions for four hours: untreated carbon dioxide (CO₂) ($n = 5$), warm humidified (whCO₂) ($n = 4$), whCO₂ with the umbilical cord exposed ($n = 3$), and whCO₂ without amniotic fluid (skin and cord exposed) ($n = 3$).

Results: *In utero* insufflation led to significant increases in fetal CO₂ and reductions in fetal pH. *Ex utero* insufflation with whCO₂ did not lead to changes in fetal blood gas measurements or cerebral perfusion parameters. Insufflation with whCO₂ with an exposed umbilical cord led to reduced umbilical blood flow.

Conclusions: Insufflation with warm humidified CO₂ with an amniotic fluid covered umbilical cord is well tolerated by the fetus without significant changes in hemodynamics or cerebral perfusion parameters.

Type of study: Basic science

Level of evidence: N/A

© 2020 Published by Elsevier Inc.

Since the 2011 publication of the landmark Management of Myelomeningocele Study (MOMS), fetal repair of myelomeningocele has become standard of care for the treatment of neural tube defects [1]. While open fetal repair improves motor and cognitive function in children, it confers an increased risk of membrane separation, preterm labor and oligohydramnios in mothers who require two laparotomies and hysterotomies over a short duration [2,3]. To reduce maternal risks, fetoscopy, a hysterotomy sparing approach, has recently been developed [4,5]. Many centers utilize partial amniotic carbon dioxide insufflation (PACI) during fetoscopic repair to overcome the challenge of

poor visibility during fetoscopy. Despite its increasing use, the effects of prolonged CO₂ insufflation on the fetus are unknown, as invasive monitoring of the human fetus during a surgical case is not feasible.

Sheep have been used to study the effects of fetoscopic intervention since their size and physiology are similar to the human fetus. Early findings from sheep studies show a strong correlation between PACI and fetal hypercapnic acidosis, but critics say differences in sheep and human placental architecture account for these effects [6,7]. Newer research also suggests that the use of heated, humidified carbon dioxide (CO₂) may mitigate some the fetal derangements observed in earlier studies [8]. Additionally, dynamic brain testing has never been used to assess the physiologic implications of these acid/base disturbances. Fetoscopic monitoring has been limited by access to the fetus. As a result, there are few proven indices of fetal status during fetoscopic procedures. Until now, a comprehensive study evaluating the safety of PACI was not possible.

Here we utilized new technologies to insufflate fetal sheep both *in utero* and *ex utero* under a variety of conditions and evaluate their metabolic and neurologic sequelae. These results allow better understanding of the optimal PACI conditions and route of fetal CO₂ absorption

[☆] Data included in this manuscript were presented in oral format at the 49th Annual American Pediatric Surgery Association in Palm Desert, California on May 3 to 6, 2018, and the Meeting of the International Society for Fetal Medicine and Surgery, in Sils, Switzerland, October 22 to 26, 2019.

* Corresponding author at: Center for Fetal Research, 3401 Civic Center Blvd., Philadelphia, PA 19104.

E-mail addresses: baracoons@gmail.com (B.E. Coons), flake@email.chop.edu (A.W. Flake).

¹ These authors contributed equally to this work.

and may ultimately have clinical implications for the field of fetoscopic surgery.

1. Materials and methods

1.1. Anesthesia protocol

All experiments were approved by the Children's Hospital of Philadelphia Research Institute Institutional Animal Care and Use Committee. After appropriate fasting and placement of transdermal fentanyl patches (2 µg/kg/h) 12 to 18 h prior to surgery, time-dated pregnant ewes were anesthetized with intramuscular ketamine (15 mg/kg) and inhaled isoflurane (1%–4% in O₂). Ventilator tidal volume (8–10 ml/kg/min) and respiratory rate [10–18] were altered to achieve a maternal end-tidal CO₂ of 35–40 mmHg and arterial CO₂ of 35–45 mmHg.

1.2. In utero protocol

1.2.1. Fetal carotid artery catheter placement

A midline laparotomy was performed on the pregnant ewe. A small hysterotomy was created, and the fetal head was exteriorized. The fetal carotid artery was cannulated via neck incision with a polyvinyl catheter (ID 0.040", Scientific Commodities, Lake Havasu, AZ). The distal aspect of the carotid catheter was secured to the ewe's flank. To secure the amniotic membranes, T-fasteners (SAF-T-PEXY T-fasteners, Halyard Health Inc, Atlanta, GA, USA) buttressed with felt pledgets (BARD Peripheral Vascular, Temple, AZ, USA) were triangulated through the uterine wall prior to hysterotomy closure. Lactated Ringer's solution treated with penicillin G (1 million units) was used to replace any lost amniotic fluid. The hysterotomy and laparotomy were then closed using sequential layers. The ewes were recovered from surgery and treated with intramuscular oxytetracycline (6 mg/kg), buprenorphine (0.005 mg/kg) and flunixin (2.5 mg/kg) for pain management. Heparinized saline (10 U/mL) was used to flush the fetal carotid catheters four times daily to ensure patency.

1.3. In utero insufflation

After 48 h of recovery, baseline fetal arterial blood gas samples (i-Stat System, Abbott Point of Care Inc., Princeton, NJ, USA) were obtained. The preoperative procedure and intraoperative anesthesia for the ewe were maintained per prior protocol. Using ultrasound guidance, a carotid arterial line was placed percutaneously in the ewe. Maternal and fetal heart rate and arterial blood pressure were monitored continuously (LabChart 7, ADInstruments Inc., Colorado Springs, CO, USA), and arterial blood gases were obtained every 20 min.

Control fetuses ($n = 3$) at gestational age (GA) 105 ± 2 days were maintained under maternal anesthesia alone. Four fetuses at GA 105 ± 1 days underwent partial amniotic fluid insufflation. For this procedure, a Veress needle (Covidien, Mansfield, MA) was inserted between prior-placed triangulated T-fasteners to access the uterus (Fig. 1). The uterus was then insufflated with untreated CO₂ to a maximum pressure of 8 mmHg (Karl Storz, Endoscopy Tuttington, Germany). Intraamniotic placement was confirmed with a 9.5 Fr cystourethroscope (Karl Storz Endoscopy, Tuttington, Germany) following exchange of the Veress needle with a 3.5 mm trocar (Aesculap Inc., Center Valley, PA, USA). To prevent overdistention of the uterus and maintain fetoplacental circulation [9], the trocar was secured and the fascia was brought together with towel clips. To approximate the length of fetoscopic myelomeningocele repair [5,10,11], both control and experimental fetuses were evaluated for four hours.

1.3.1. Histology

After four hours, fetuses were euthanized (pentobarbital sodium 117 mg/kg and phenytoin sodium 15 mg/kg) and their brains were perfusion fixed with 10% formalin [12]. The cerebrum and cerebellum were

removed from the skull and submerged in formalin for 10–14 days. Coronal slices (10mm) of the forebrain and cerebellum were cut using a brain matrix (Ted Pella Inc, Redding, CA, USA), embedded in paraffin and sectioned at 5 µm. Hemorrhagic lesions were assessed on hemotoxylin and eosin (H&E) stained slides.

Anatomically equivalent sections from the frontal lobe and cerebellum were reacted with antibodies. Astroglia were visualized with rabbit glial fibrillary acidic protein (GFAP) antisera (1:400, Z-0334; DAKO, Carpinteria, CA). Microglia were visualized with a rabbit anti-ionized calcium-binding adaptor molecule 1 (Iba-1) antibody (1:1000, 178846; ABCam, Cambridge, MA, USA). Apoptotic cells were visualized with rabbit caspase antibody (1:100, ab4051, Abcam, Cambridge, MA, USA). Sections were incubated overnight with antirabbit secondary antibody (1:500, ThermoFisher, Waltham, MA, USA) and developed with horseradish peroxidase (SK-410; Vector Laboratories, Burlingame, CA, USA). Slides were scanned at 20× magnification and evaluated using Aperio Imagescope Version 12.3 (Leica Biosystems, Buffalo Grove IL, USA).

Comparative morphometric analyses were performed on homologous and anatomically-matched sections. Specific neuroanatomic landmarks, including the anterior horn of the lateral ventricle and inferior cerebellar peduncle, were used to select frontal lobe and cerebellar sections, respectively. In the frontal lobe, periventricular white matter boundaries were defined by a horizontal line drawn tangent to the lateral ventricle at the head of the caudate nucleus, connecting to the fundi of adjacent sulci, and the white matter boundaries at those fundi [13]. Grey matter was evaluated at the level adjacent to these boundaries. Quantitative measures described below reflect these white and gray matter regions of interest (ROIs). ROIs were analyzed at 5× magnification in 3 fields (76.9 mm²), and the mean values of these quantifications were compared between groups. Area fraction of Iba-1-positive microglia and astrocyte-positive GFAP were calculated within each ROI using a calibrated color deconvolution algorithm (Aperio Technologies, Buffalo Grove, IL, USA) [14,15]. The areas of positive staining were subtracted from the total areas of the high powered fields studied and expressed as a percentage (%).

For detection of apoptotic cells, Caspase-3 positive cells were manually counted in ROIs. In addition to cortical ROIs, cerebellar white matter and gray matter were also analyzed for caspase-positive cells.

1.4. Ex utero protocol

1.4.1. Surgical procedure for cannulation onto EXTEND for ex utero studies

A lower midline laparotomy was created, and the uterine horns were exteriorized with care. A hysterotomy was performed, and the fetus is given one intramuscular dose of vecuronium (0.004–0.008 mg/kg). The fetus was then removed from the uterus, taking care to avoid tension placed on the umbilical cord. The umbilical cord is dissected, and the umbilical vein cannulated, followed by the two umbilical arteries. All vessels were cannulated using custom made 12Fr cannula tips, and connected to a pumpless circuit with a Maquet Quadrox-ID Pediatric Oxygenator. The fetus was then enclosed in an insufflation-capable Biobag. Animals were able to recover for a minimum of twenty-four hours, during which circuit flows and lab values stabilized, before undergoing insufflation. Fetal parameters such as temperature, preoxygenator mean arterial pressure, postoxygenerator mean arterial pressure, heart rate, circuit flow, and oxygen saturations were recorded continuously using the LabChart 7 and PowerLab data acquisition system (AD Instruments, Colorado Springs, Colorado, USA).

1.5. Ex utero insufflation procedure

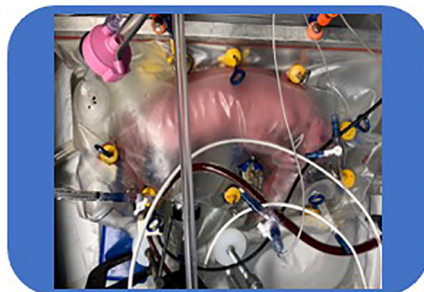
Next, we sought to isolate the effects of insufflation on the fetus from the confounding effects of the cotyledonary placenta by performing ex utero insufflation. After the cannulation surgery described above, four individual fetuses underwent ex utero insufflation to 8 mmHg. We



In Utero Insufflation

In Utero Insufflation

- n = 3
- Partial Amniotic CO₂ Insufflation



Ex Utero Insufflation

Untreated CO₂

- n = 5
- Partial Amniotic CO₂ Insufflation

Warm, Humidified CO₂

- n = 4
- Partial Amniotic CO₂ Insufflation

Uncovered Umbilical Cord

- n = 3
- Partial Amniotic CO₂ Insufflation, but with Cord Exposed

Total Amniotic CO₂ Insufflation

- n = 3
- Cord Exposed

Fig. 1. Experimental schematic.

utilized a boxcar experimental design, in which each individual fetus is exposed to alternating experimental conditions [16]. This experimental design is demonstrated in Fig. 2. The four conditions we used were: untreated carbon dioxide (CO₂), warm humidified (whCO₂), whCO₂ with the umbilical cord exposed, and whCO₂ without amniotic fluid (skin and cord exposed) (Fig. 1). These conditions were chosen to contrast the physiologic effects between dry and whCO₂, and to investigate differing degrees of umbilical cord and fetal skin exposure.

In the untreated CO₂ group and the warm humidified CO₂ group, the partial amniotic carbon dioxide insufflation (PACI) technique was utilized. The amniotic fluid level was adjusted to cover approximately half of the fetal skin and the umbilical cord during insufflation limiting direct CO₂ exposure to the surface area of half the fetal skin. Next, we sought to investigate the effect of uncovering the umbilical cord. In the whCO₂ with the umbilical cord exposed group, insufflation was initiated in an identical manner to previous experiments with whCO₂. After 60 min of insufflation, the cord was uncovered from the amniotic fluid solution keeping the fetal skin half submerged. This experiment was designed to test the effect of CO₂ absorption through the umbilical cord membranes. In the whCO₂ without amniotic fluid group, there was no amniotic fluid in the Biobag during insufflation and the fetal skin and umbilical cord were completely exposed. This was meant to test for CO₂ absorption across fetal skin.

During these experiments, a Karl Storz Thermoflator (Model Number 264320-20) was attached to the Biobag using a Luer lock compatible port. Untreated CO₂ was conveyed via high-flow insufflation tubing (22 M/10 M). Warmed, humidified CO₂ was conditioned by an Insufflow Lexion Device (Model Number 6198-SC) with accompanying specialized high-flow tubing (Reference Number 6198). Each insufflation period was four hours, and pressure was maintained at 7–8 mmHg, a number chosen as it mimics clinical conditions. Animals were allowed twenty-four hours to sufficiently recover between each exposure, as judged by normalization of hemodynamic status and laboratory values.

1.5.1. Laboratory values

All laboratory values were measured using I-Stat 1 Analyzers (Model Number 300-G, Abbott Point of Care Inc., Princeton, NJ, USA). We used CG4 cartridges to assess pH, pCO₂, pO₂, Lactate, Base Excess, and bicarbonate (Product number 03P85-50).

1.5.2. Contrast-enhanced ultrasound examinations

Brain parenchymal perfusion was evaluated using contrast-enhanced ultrasound (CEUS). All examinations were performed by a board-certified pediatric radiologist every twenty to thirty minutes through the sonolucent Biobag. Lumason® (sulfur hexafluoride lipid-type A microspheres; Bracco Diagnostics Inc., Monroe Township, NJ, USA) ultrasound contrast agent was prepared per manufacturer guidelines. A 0.2 mL bolus was administered on the postoxygenator limb of the EXTEND circuit. Concurrent 90-s cine clip acquisition was obtained in a transaxial plane with visualization of the thalami. Images were obtained using a commercially-available GE Logiq E9 ultrasound system

(GE Healthcare, Waukesha, WI, USA) and a C2-9 MHz transducer with settings optimized for contrast visualization.

VueBox™ (Bracco Imaging Suisse SA, Geneva, Switzerland) was used for analysis (AS) after creating regions of interest (ROIs) which included the entire brain and excluded the fetal skull. Following generation of time-intensity-curves, perfusion metrics including rise time (RT), fall time (FT), and transit time (TT) were extrapolated [17–19]. Studies were included if quality-of-fit of the curve-fitting model was greater than or equal to 80%.

1.5.3. Data acquisition and formulas

Fetal blood pressure, heart rate, circuit blood flow rates, transmembrane pressure differential, sweep gas flow and incubator fluid temperature were continuously recorded (LabChart 7, ADInstruments Inc.).

$Postmembrane\ oxygen\ content = (1.34 * Hgb * postmembrane\ oxygen\ saturation) + (0.0031 * postmembrane\ PaO_2)$.

$Premembrane\ oxygen\ content = (1.34 * Hgb * premembrane\ oxygen\ saturation) + (0.0031 * premembrane\ PaO_2)$.

$Weight-adjusted\ circuit\ flow = absolute\ circuit\ flow / estimated\ daily\ weight$.

$Oxygen\ delivery\ (ml\ kg^{-1}\ min^{-1}) = weight-adjusted\ circuit\ flow * postmembrane\ oxygen\ content$.

$Oxygen\ consumption\ (ml\ kg^{-1}\ min^{-1}) = weight-adjusted\ circuit\ flow * (postmembrane\ oxygen\ content - premembrane\ oxygen\ content)$.

$Oxygen\ extraction\ (\%) = (oxygen\ consumption / oxygen\ delivery) * 100\%$.

Estimated daily weight. Growth rate was assumed to be exponential and derived from measured body weight at the start and end of each run (according to the formula $y = ae^{bx}$, where 'a' is starting weight and 'b' is growth rate in $g\ kg^{-1}$ per day). Estimated daily weights (for weight-adjusted calculations) were extrapolated from the exponential growth rate calculated for each lamb.

1.6. Statistical analysis

Statistical analysis was performed using GraphPad Prism 5.0 (Prism, GraphPad Software, Inc. La Jolla, CA) and Stata/IC 15.1. For *in utero* experiments, maternal and fetal hemodynamic parameters (heart rate and blood pressure) and arterial blood gas measurements were compared over time using two-way repeated measure analysis of variance (ANOVA). CEUS perfusion metrics were compared between groups with two-tailed unpaired Student's t-test at matched time points. Histologic parameters were quantified in triplicate, and mean values compared with a two-tailed unpaired Student's t test. For *ex utero* experiments, hemodynamic parameters and arterial blood gas measurements were compared over time with a two-way repeated measures ANOVA. The relationship between CEUS perfusion parameters and fetal arterial CO₂ and pH levels was determined by a mixed linear regression analyses with random intercepts by animal and date of study. All data are presented as mean ± standard error of the mean unless otherwise specified. Significance was accepted at $p < 0.05$.

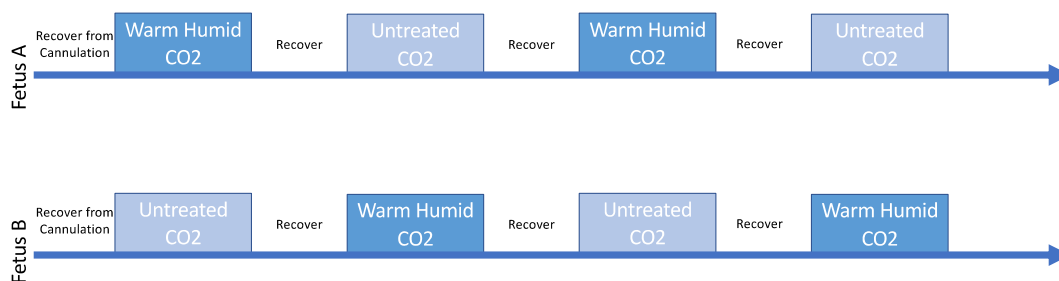


Fig. 2. Ex utero insufflation technique and the use of the boxcar experimental design. Each fetus is 104–107 days gestational age. The recovery period is twenty-four hours and the normalization of all laboratory values.

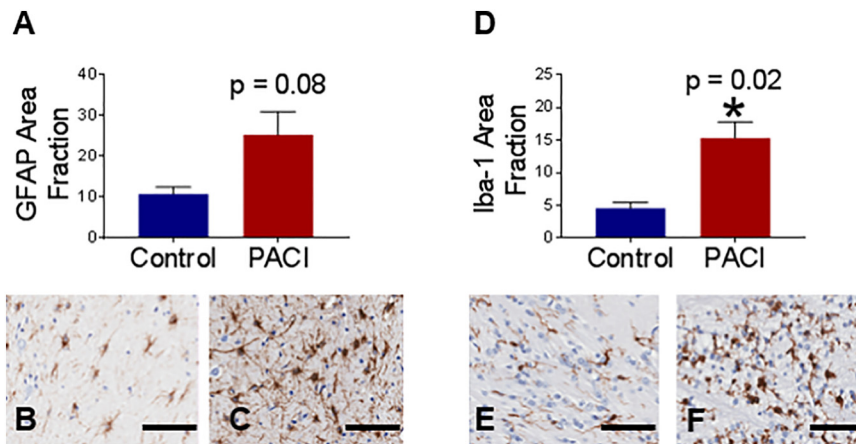


Fig. 3. Frontal lobe periventricular white matter from noninsufflated control fetuses (B) had a trend toward fewer GFAP-labeled astrocytes than insufflated fetuses ($p=0.08$) but the difference did not reach statistical significance. (C). $5\times$, scale bar = $100\ \mu\text{m}$. (E) In frontal lobe periventricular white matter, Iba-1-labeled microglia (D) were significantly reduced in noninsufflated control fetuses (E) versus insufflated fetuses (F) ($p=0.02$). $5\times$, scale bar = $100\ \mu\text{m}$.

2. Results

2.1. In utero

2.1.1. In utero insufflation in ovine model shows decreased pH and increased $p\text{CO}_2$

Compared to noninsufflated fetuses, insufflated fetuses had significantly decreased pH levels and significantly increased arterial CO_2 levels (Fig. 1 A–B). There was no difference in fetal arterial oxygen levels between noninsufflated and insufflated fetuses throughout the study period (Fig. 1C). Fetal heart rate (Fig. 1D) and mean arterial pressure (40 ± 6 vs. 42 ± 3 mmHg, $p=0.73$) were also maintained with no difference between groups throughout the anesthesia period.

2.1.2. Histologic data

No hemorrhage or infarcts were identified in reviewed cerebral or cerebellar sections from *in utero* animals. Insufflated and control fetuses had no differences in quantities of caspase-3 positive apoptotic cells in the cerebellum (1.2 ± 0.2 vs. 0.7 ± 0.5 cells/hpf, $p=0.4$), periventricular white matter (0.6 ± 0.3 vs. 0 cell/hpf, $p=0.1$), or cortical gray matter (0.1 ± 0.1 vs. 0 cell/hpf, $p=0.4$).

The area fraction stained for GFAP-labeled astrocytes was increased in the frontal lobe white matter of insufflated fetuses compared to noninsufflated fetuses, although this was not significant (25 ± 6 vs. $11 \pm 2\%$, $p=0.08$) (Fig. 3A–C). The area fraction stained for Iba-1-labeled microglia was significantly elevated in the frontal lobe white matter of insufflated fetuses (15 ± 2 vs. $5 \pm 1\%$, $p=0.02$) (Fig. 3D–F).

2.2. Ex utero

2.2.1. Warm, humidified CO_2 yields less $p\text{CO}_2$ and pH change

In the EXTEND system, insufflation with wh CO_2 led to less change in $p\text{CO}_2$ and pH when compared with untreated CO_2 (Fig. 4A–D). There was no noticeable difference in blood flow or heart rate between the two groups.

2.2.2. Exposing the umbilical cord during insufflation decreases blood flow

We did not find any statistically significant difference in the pH and $p\text{CO}_2$ once the cord was uncovered; however, we did see a statistically significant decrease in blood flow through the umbilical cord once it was exposed (Fig. 5A–D, $p=0.046$). Additionally, the oxygen delivery was decreased, but not to a statistically significant degree (Fig. 5D, $p=0.165$).

2.2.3. Total amniotic CO_2 insufflation does not affect pH or PCO_2 but similarly reduces umbilical blood flow

Once we exposed the umbilical cord, we next sought to find out if there was any further effect of exposing all of the fetus' skin to CO_2 . However, total amniotic CO_2 insufflation had similar effects as solely exposing the umbilical cord: blood flow was significantly reduced ($p=0.0460$, Fig. 6C), but pH and $p\text{CO}_2$ were not affected (Fig. 6A–D). Oxygen delivery was once again decreased, but not to a significant degree (Fig. 6D, $p=0.086$).

2.2.4. CEUS brain perfusion parameters correlate with serum pH and $p\text{CO}_2$

A total of 117 CEUS studies were adequate for quantification and analysis. Mixed effect linear regression analyses demonstrated statistically significant correlations between brain perfusion parameters and serum pH and $p\text{CO}_2$ levels. With increased $p\text{CO}_2$ levels, there were decreased rise time (RT) ($p<0.001$), fall time (FT) ($p=0.022$), and transit time (TT) ($p=0.003$) (Fig. 7). Correspondingly, with decreased pH levels, there were decreased RT ($p=.002$), FT ($p=0.047$), and TT ($p=0.012$). This decrease in time parameters is thought to reflect increased cerebral blood flow secondary to localized vasodilation in the setting of hypercapnic acidosis.

3. Discussion

Previous studies of the effects of insufflation on fetuses, conducted in the sheep model, were confounded by the cotyledonary nature of the ovine placenta. We validated prior results in an *in utero* model and demonstrated marked fetal hypercapnic acidosis. When isolating the fetus from the placenta in *ex utero* insufflation studies in the EXTEND system we found less aberration in fetal blood gases suggesting that placental absorption influences fetal $p\text{CO}_2$ and pH levels. Furthermore, we found that using warm, humidified CO_2 was safer for the fetus. Exposure of the umbilical cord and fetal skin does not affect fetal $p\text{CO}_2$ or pH, indicating that the umbilical cord and fetal skin do not serve as a pathway for CO_2 absorption.

One advantage of the *ex utero* system is the ability to control the degree to which the fetus is exposed. In previous studies, all of which have been *in utero*, partial amniotic carbon dioxide insufflation was used. However, the ovine uterus is much thinner than a human uterus, and much more distensible. As a result, *in utero* insufflation in the ovine uterus is much more difficult to control and may have greater effects on uterine and placental blood flow. Using the *ex utero* model, we performed a stepwise approach to understanding the effects of CO_2 insufflation on the isolated fetus independent of maternal uterine or placental factors.

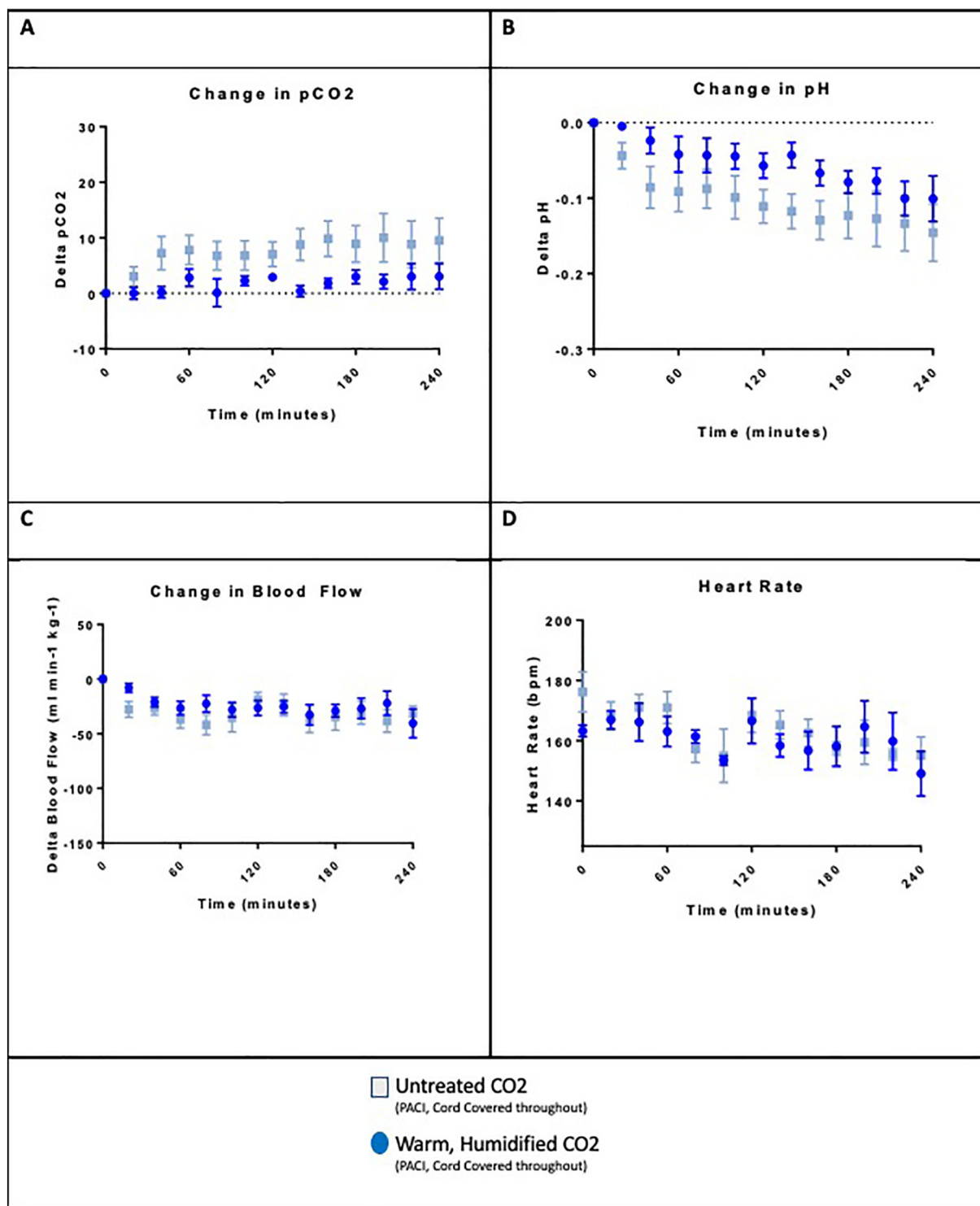


Fig. 4. Untreated CO₂ versus warm, humidified CO₂ modeled in the EXTEND system. Untreated CO₂ insufflation led to greater increases in pCO₂ (A) and larger decreases in pH (B). There were no significant effects on blood flow (C) or heart rate (D).

First, we validated recent work performed *in utero* by Amberg et al [8], by comparing warm, humidified CO₂ insufflation to untreated CO₂ in our *ex utero* system. Though we noted that warm, humidified CO₂ was safer for the fetus, we did not see the acidemia or hypercapnia noted by Amberg et al *in utero*. We theorize that this is because of the fact that *ex utero*, abnormalities of uterine/placental blood flow do not occur and the cotyledons are no longer present, so their absorption of CO₂ can no longer affect fetal acid–base balance.

We also expanded on Amberg et al's work by examining fetal brain histology during *in utero* PACI. We showed that fetal brain had no significant differences in caspase-3 positive cells in the cerebellum, periventricular white matter, or cortical gray matter. Thus when “placental” bloodflow remains normal, fetoscopic insufflation appears to be safe for the developing fetal brain. However, we do see that at necropsy, insufflated fetuses had increased astrocyte (25 ± 6 vs. 11 ± 2%, p = 0.08) and microglial (15 ± 2 vs. 5 ± 1 %, p = 0.02) cell densities in frontal lobe white matter without hemorrhage or elevations in cellular

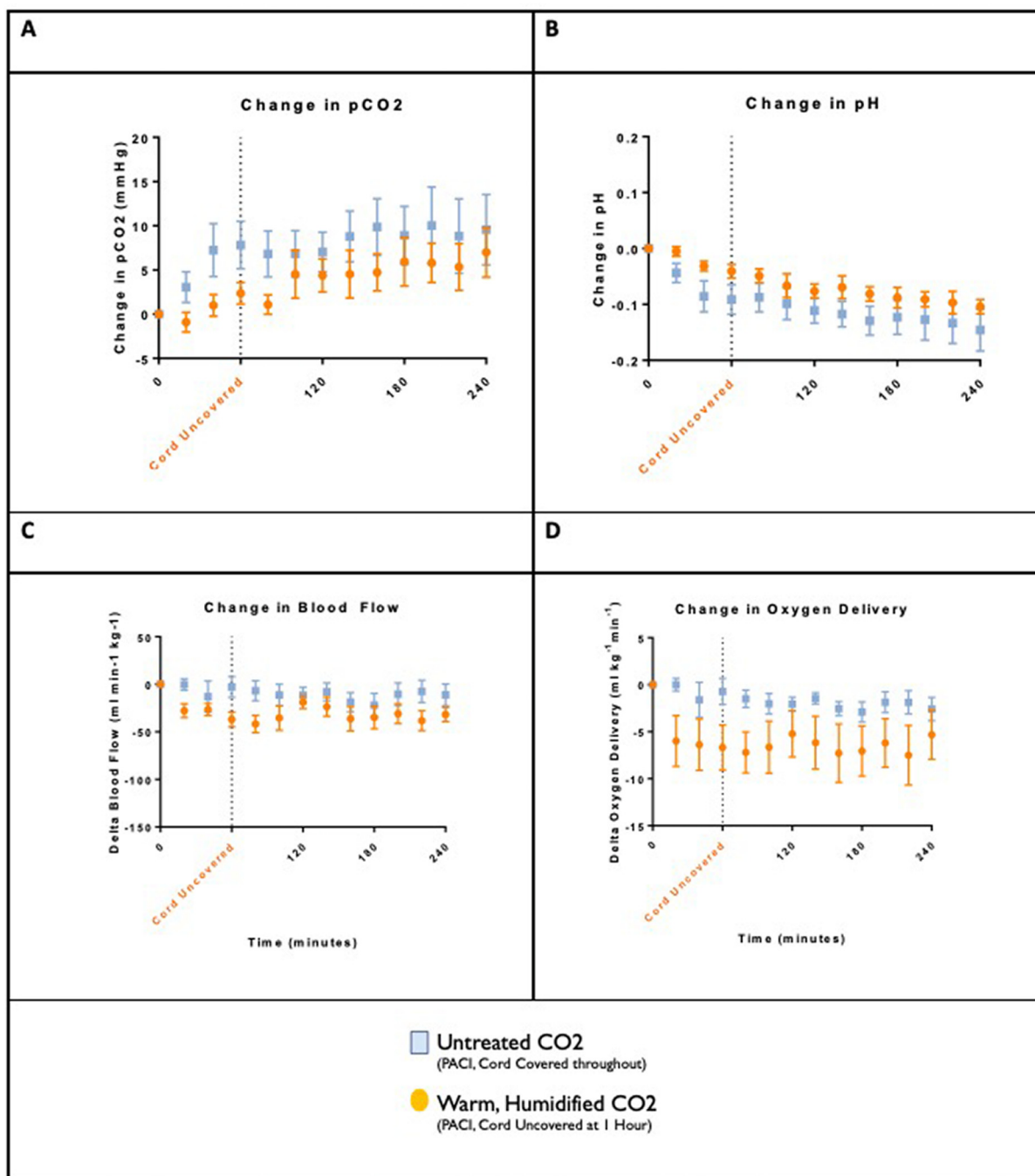


Fig. 5. The effects of uncovering the umbilical cord as modeled in the EXTEND system. Uncovering the umbilical cord does not lead to changes in pCO₂ (A) or pH (B), but it does decrease blood flow (C), and as a result of decreased blood flow, oxygen delivery to the fetus drops as well (D).

apoptosis compared to controls. This represents a gliocyte activation or possibly an inflammatory response and is likely secondary to increased pCO₂ as a result of increased carbon dioxide absorption across the *in utero* ovine cotyledonary system. As a result, we turned to the EXTEND model to evaluate effects without the ovine placenta.

By using EXTEND, we sought to truly isolate the effects of umbilical cord exposure using the *ex utero* model. When the cord was exposed, we noted a statistically significant decrease in blood flow. Oxygen delivery also dropped, but not to a statistically significant level. Nonetheless, the pH and pCO₂ did not significantly deviate from unexposed cord values. This indicates that although the temperature changes and pressure changes of cord exposure may decrease blood flow, there is no CO₂ absorption across fetal umbilical

cord membranes. Likewise, the whCO₂ without amniotic fluid (skin and cord exposed) insufflation experiments showed that exposure of all fetal skin, mucocutaneous membranes, and the umbilical cord did not have any effect on pCO₂. This indicates that there is no percutaneous absorption of CO₂.

Prior studies have been unable to monitor the effects of fetoscopic insufflation on fetal brain perfusion. In this study, we utilized emerging ultrasonographic technologies to evaluate fetal brain perfusion with CEUS. Similar to MRI perfusion and CT perfusion, CEUS extrapolates perfusion parameters which help characterize localized changes in cerebral blood flow. We demonstrate that in the EXTEND system, brain perfusion parameters strongly correlate with fetal serum pCO₂ and pH levels. Less aberrations in brain perfusion parameters are seen with more

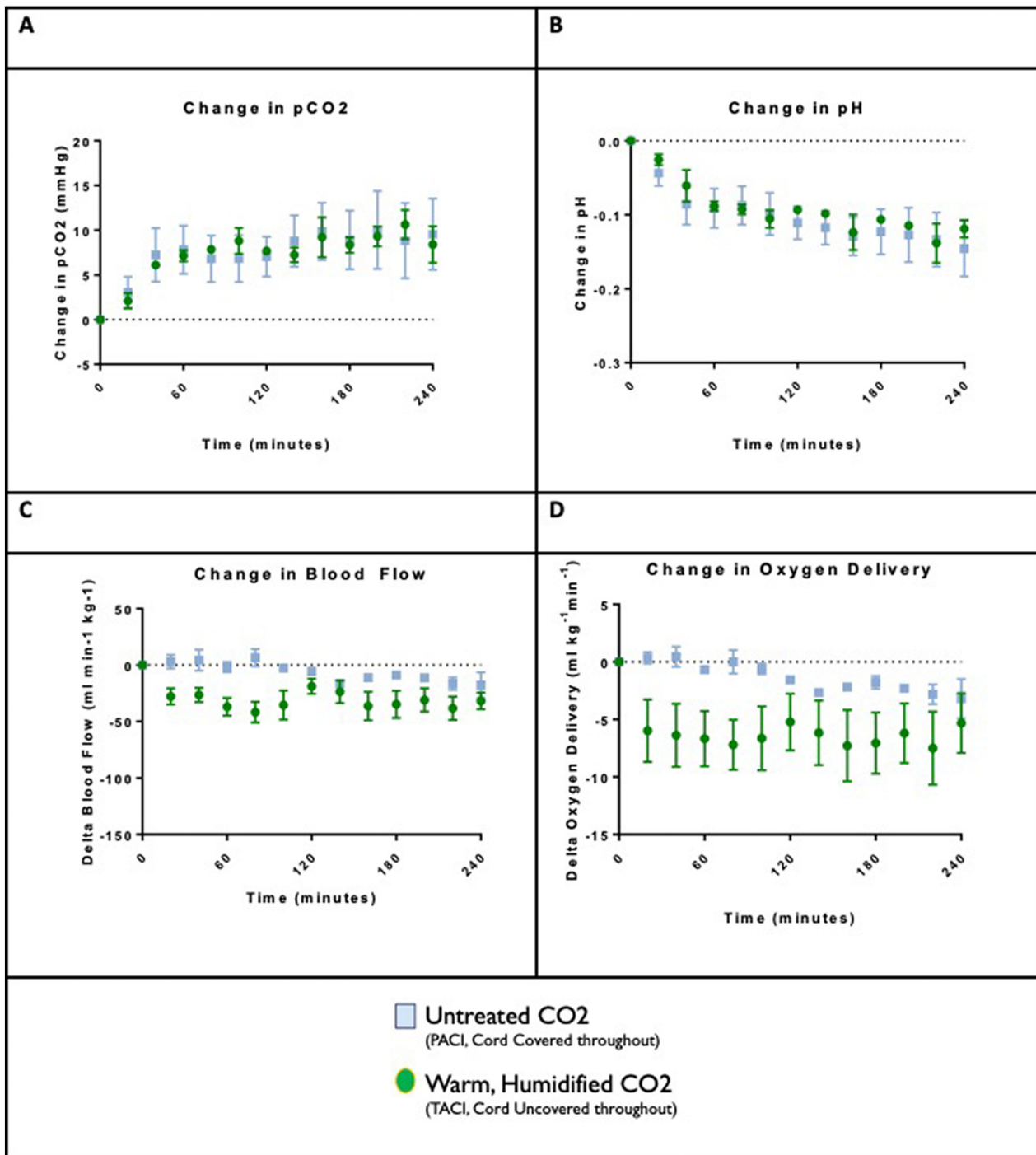


Fig. 6. TACI: total amniotic CO₂ insufflation modeled in the EXTEND system. When the animal is fully exposed to insufflation, there is no effect on pCO₂ (A) or pH (B), but there is a decrease in blood flow of the umbilical cord (C) and resultant oxygen delivery (D).

normalized pH and pCO₂ levels, further highlighting the importance of keeping fetal acid–base status physiologic. Current fetal monitoring during fetoscopic surgery is predominately with fetal echocardiography [20]. However, this modality has limited utility in evaluating fetal brain perfusion aberrations especially considering the documented stability of fetal heart rate and oxygenation in our *in utero* and *ex utero* studies. As hypercapnic acidosis is reflected in the perfusion metrics, CEUS may serve as a useful tool in the future for fetal monitoring in experimental and clinical interventions. Our key finding, which showed that as pCO₂ levels increased, there was a decrease in RT, FT, and TT suggests that these three indices can be used as a non-invasively obtained proxy for fetal hypercapnia. As more fetoscopic interventions are

performed, the use of these indices will be an important bellweather for fetal distress.

One limitation of this study is the small sample size. Unfortunately, this limitation was dictated by the expense and difficulty of performing large animal experiments. We tried to maximize resources by using a boxcar experimental design (as highlighted in Fig. 2); however, owing to the small sample size, type II errors are more likely to occur. Owing to the effects of small sizes, the independent variable effect is small, and variability is large.

The data in this study strongly support the use of warm humidified CO₂ in fetoscopic surgery. It also supports keeping the umbilical cord submerged in amniotic fluid during insufflation and

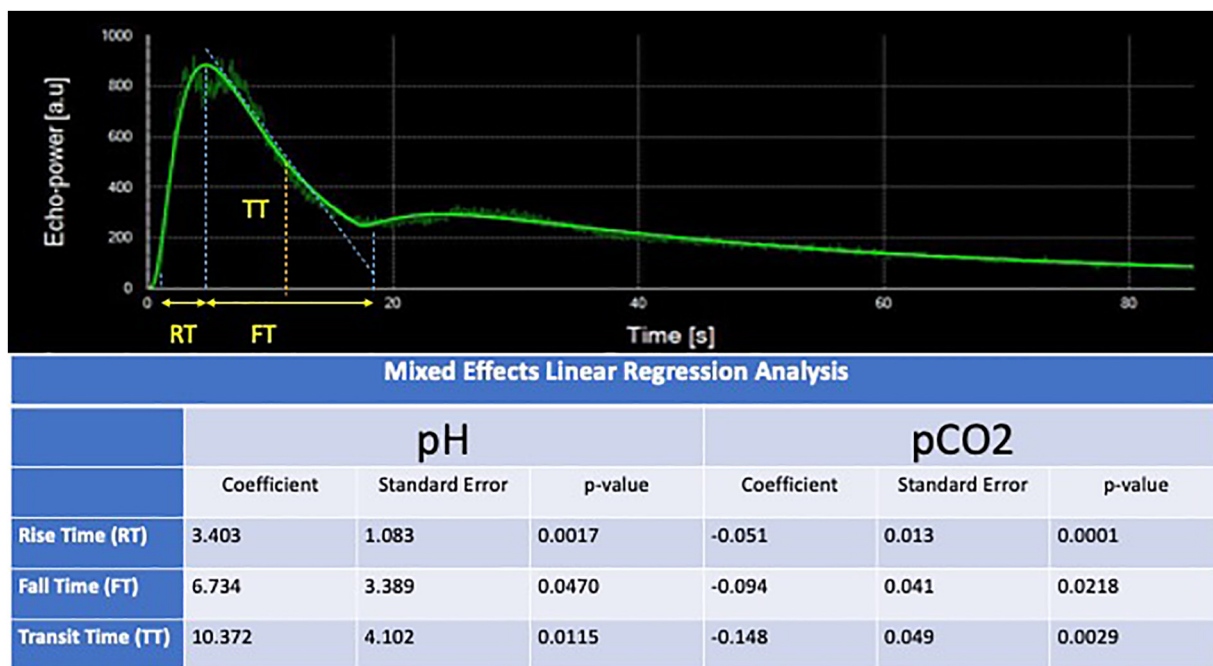


Fig. 7. Associations between brain perfusion parameters by contrast-enhanced ultrasound and serum pH and pCO₂ from mixed effect linear regression analyses illustrated by corresponding p-values. A representative time intensity curve, or TIC, is provided and labeled with rise time (RT), fall time (FT), and transit time (TT). As pCO₂ levels increased, there was a decrease in RT (p<0.001), FT (p=0.022), and TT (p=0.003) (Fig. 7). Furthermore, decreased pH levels also corresponded to decreased RT (p=.002), FT (p=0.047), and TT (p=0.012).

indicates that fetal skin exposure does not result in significant CO₂ absorption.

Acknowledgment

We would like to acknowledge the contributions of Grace Hwang, Haley Peterson, Ashley Spina, Christian Reice, Stelios Monos, Jacqueline Amato, and Aaron Weilerstein in the support of this project.

Statement of ethics

Research was conducted at Children’s Hospital of Philadelphia under IACUC Protocol IAC 16-001212.

Disclosure statement

Dr. Alan Flake and Dr. Marcus Davey are patent holders on the EXTEND system.

Funding sources

The research presented in this paper was supported by a TL1 TR001880. Research reported in this publication was supported by the National Center for Advancing Translational Sciences of the National Institutes of Health under Award Number TL1TR001880 and Award Number UL1TR001878. The content is solely the responsibility of the authors and does not necessarily represent the official views of the NIH. Supported in part by the Institute for Translational Medicine and Therapeutics (ITMAT) Transdisciplinary Program in Translational Medicine and Therapeutics. This work was also supported in part by the Children’s Hospital of Philadelphia Research Institute and Department of Radiology.

Appendix A. Supplementary data

Supplementary data to this article can be found online at <https://doi.org/10.1016/j.jpedsurg.2020.09.029>.

References

- [1] Adzick NS, Thom EA, Spong CY, et al. A randomized trial of prenatal versus postnatal repair of myelomeningocele. *N Engl J Med.* 2011;364(11):993–1004.
- [2] Farmer DL, Thom EA, Brock JW, et al. The management of myelomeningocele study: full cohort 30-month pediatric outcomes. *Am J Obstet Gynecol.* 2018;218(2):256.e1–256.e13.
- [3] Johnson MP, Bennett KA, Rand L, et al. The management of myelomeningocele study: obstetrical outcomes and risk factors for obstetrical complications following prenatal surgery. *Am J Obstet Gynecol.* 2016;215(6):778.e1–9.
- [4] Belfort M, Whitehead W, Shamshirsaz A, et al. Fetoscopic repair of meningocele. *Obstet Gynecol.* 2015;126(4):881–4.
- [5] Belfort MA, Whitehead WE, Shamshirsaz AA, et al. Fetoscopic open neural tube defect repair: development and refinement of a two-port, carbon dioxide insufflation technique. *Obstet Gynecol.* 2017;129(4):734–43.
- [6] Luks FI, Deprest J, Marcus M, et al. Carbon dioxide pneumoamnios causes acidosis in fetal lamb. *Fetal Diagn Ther.* 1994;9(2):105–9.
- [7] Pelletier GJ, Srinathan SK, Langer JC. Effects of intraamniotic helium, carbon dioxide, and water on fetal lambs. *J Pediatr Surg.* 1995;30(8):1155–8.
- [8] Amberg BJ, Hodges RJ, Kashyap AJ, et al. Physiological effects of partial amniotic carbon dioxide insufflation with cold, dry vs heated, humidified gas in a sheep model. *Ultrasound Obstet Gynecol.* 2019;53(3):340–7.
- [9] Skarsgard ED, Bealer JF, Meuli M, et al. Fetal endoscopic (‘Fetendo’) surgery: the relationship between insufflating pressure and the fetoplacental circulation. *J Pediatr Surg.* 1995;30(8):1165–8.
- [10] Ziemann M, Fimmers R, Khaleeva A, et al. Partial amniotic carbon dioxide insufflation (PACI) during minimally invasive fetoscopic interventions on fetuses with spina bifida aperta. *Surg Endosc.* 2018;32(7):3138–48.
- [11] Pedreira DAL, Zanon N, Nishikuni K, et al. Endoscopic surgery for the antenatal treatment of myelomeningocele: the CECAM trial. *Am J Obstet Gynecol.* 2016;214(1):111.e1–111.e11.
- [12] Hutton LC, Castillo-Melendez M, Smythe GA, et al. Microglial activation, macrophage infiltration, and evidence of cell death in the fetal brain after uteroplacental administration of lipopolysaccharide in sheep in late gestation. *Am J Obstet Gynecol.* 2008;198(1):117.e1–11.
- [13] Riddle A, Luo NL, Manese M, et al. Spatial heterogeneity in oligodendrocyte lineage maturation and not cerebral blood flow predicts fetal ovine periventricular white matter injury. *J Neurosci.* 2006;26(11):3045–55.
- [14] Ruifrok AC, Johnston DA. Quantification of histochemical staining by color deconvolution. *Anal Quant Cytol Histol.* 2001;23(4):291–9.

- [15] Helps SC, Thornton E, Kleinig TJ, et al. Automatic nonsubjective estimation of antigen content visualized by immunohistochemistry using color deconvolution. *Appl Immunohistochem Mol Morphol*. 2012;20(1):82–90.
- [16] Demaerel P. Recent advances in diagnostic neuroradiology. Springer; 2013 525 p.
- [17] Vinke EJ, Kortenbout AJ, Eyding J, et al. Potential of contrast-enhanced ultrasound as a bedside monitoring technique in cerebral perfusion: a systematic review. *Ultrasound Med Biol*. 2017;43(12):2751–7.
- [18] Hwang M, De Jong RM, Herman S, et al. Novel contrast-enhanced ultrasound evaluation in neonatal hypoxic ischemic injury: clinical application and future directions. *J Ultrasound Med*. 2017;36(11):2379–86.
- [19] Kastler A, Manzoni P, Chapuy S, et al. Transfontanellar contrast enhanced ultrasound in infants: initial experience. *J Neuroradiol*. 2014;41(4):251–8.
- [20] Rychik J, Tian Z, Cohen MS, et al. Acute cardiovascular effects of fetal surgery in the human. *Circulation*. 2004;110(12):1549–56.